

## A neutron reflection study of adsorbed deuterated myoglobin layers on hydrophobic surfaces

Nicolas Brouette<sup>a</sup>, Giovanna Fragneto<sup>b</sup>, Fabrice Cousin<sup>c</sup>, Martine Moulin<sup>b</sup>, Michael Haertlein<sup>b</sup>, Michele Sferrazza<sup>a,\*</sup>

<sup>a</sup> Département de Physique, Faculté des Sciences, Université Libre de Bruxelles, Boulevard du Triomphe, CP223, B-1050 Bruxelles, Belgium

<sup>b</sup> Institut Max Von Laue-Paul Langevin, F-38042 Grenoble, France

<sup>c</sup> Laboratoire Léon Brillouin, CEA Saclay, Gif sur Yvette 91191 Cedex, France

### ARTICLE INFO

#### Article history:

Received 22 August 2012

Accepted 15 September 2012

Available online 26 September 2012

#### Keywords:

Protein adsorption  
Hydrophobic surface  
Neutron reflectivity  
Protein unfolding

### ABSTRACT

The structure of adsorbed globular protein layers on hydrophobic surfaces is elucidated in detail by combining the use of a fully deuterated protein, myoglobin, and the neutron reflectivity technique. The hydrophobic surfaces consist of grafted self-assembled monolayer of octadecyltrichlorosilane (OTS) and polystyrene (PS) layer on silicon substrates. Different protein concentrations ranging from 1 mg/ml to 0.01 mg/ml are used. On the OTS surface and for low protein concentration, the adsorbed protein layer consists of a dense layer of thickness around 13 Å indicating that proteins are denatured when adsorbed on the hydrophobic interface – myoglobin being a globular protein with an average diameter of about 40 Å. At high protein concentration, an additional layer is observed on the top of this first denatured layer. The thickness of this layer corresponds roughly to the dimensions of the myoglobin suggesting that additional proteins in their bulk conformation are adsorbed on the top. In the case of PS, the protein is significantly less flattened at the interface, PS being a less hydrophobic surface.

© 2012 Elsevier Inc. All rights reserved.

### 1. Introduction

Protein adsorption on solid surfaces in contact with an aqueous environment has been a very active field of research for the last few decades: the understanding of the different aspects of the process is a crucial step for many practical applications with many ramifications in different disciplines, from the use of protein for colloid stabilization, development of surgical implants and biosensors, functioning of cell membranes to mention some [1,2]. The adsorption process is a complex phenomenon driven by surface-protein interactions – van der Waals forces, electrostatic and hydrophobic interactions [3,4]. It depends also on the structure and stability of the protein, the nature of the protein solution (for example pH, ionic strength, protein concentration, temperature) and surface properties (hydrophobicity, chemical composition, etc.) [5]. Adsorption on hydrophilic silicon surfaces is related to the electrostatic interaction between the protein and the surface [6,7] and thus depends on the charge of the protein which itself varies with the isoelectric point (PI) and pH [8–11]. Van der Waals interactions may also have non-negligible effects on the adsorption, as illustrated recently [12]. Protein adsorption on surfaces can be repressed, on the other hand, by hydrophilic polymer

brushes due to osmotic penalty for protein insertion into the brush [13–15]. Indeed, surfaces coated with polyethylene glycol (PEG) brushes are known to reduce the amount of adsorbed protein depending on the grafting density and also on the bulk protein concentration [16–19]. On hydrophobic surfaces, protein adsorption is supposed to be dominated by hydrophobic interactions leading to protein denaturation [1]. This denaturation is attributed to the strong affinity of the hydrophobic surface for the hydrophobic fragments within the protein. Of particular interest are any conformational changes undergone by the protein molecules upon adsorption, and the role of these in determining the structure and behavior of the adsorbed layer. Not only do such changes often play a decisive role in the energetics and kinetics of adsorption, they may also provide a valuable insight into the understanding of the process by which a globular protein adopts its unique native state. In general, proteins alter their conformation more on hydrophobic surfaces than on hydrophilic ones [20,2]. This is in order for the contact of the protein's hydrophobic residues with the like surface to be maximized, and may be revealed by the native shape of the molecule “squashing” upon adsorption to hydrophobic surfaces. A better understanding of the effects of adsorption on protein conformation may also have important implications in the field of immunology, where the use of antibody-antigen assays involving the adsorption of protein antigen onto a solid surface are seeing widespread use [21,22].

\* Corresponding author.

E-mail address: msferraz@ulb.ac.be (M. Sferrazza).

Protein adsorption at solid/liquid interfaces has been widely studied using a variety of experimental techniques such as ellipsometry, Surface Plasmon Resonance (SPR), Quartz Crystal Microbalance (QCM), radiolabeling, fluorescence microscopy, neutron reflection, circular dichroism and infrared spectroscopy. Although SPR, QCM and radiolabeling allow determining the protein adsorbed amount, they cannot establish the structure of the adsorbed layer. On the reverse, circular dichroism and infrared spectroscopy allow probing the change of secondary and tertiary structure of the protein upon adsorption but they do not give information on the adsorbed amount [23]. Finally, neutron reflectivity is a technique, which allows simultaneously to determine the thickness and the volume fraction of the adsorbed protein layers leading to the adsorbed amount [24]. It is then possible to identify if the adsorbed proteins retain their native structure or are denaturated at interfaces.

In our study, we explore the effect of protein concentration on the structure of the adsorbed layers on different hydrophobic surfaces. The use of neutron reflectometry combined with deuterated protein allows us to be highly sensitive to protein structure layer changes at the interface: we observe a thin dense layer adsorbed at low protein concentration and a two-layer structure at higher concentration. The structure of the protein layer depends also on the hydrophobicity of the surface. Fully deuterated myoglobin, a small heme protein found abundantly in vertebrate muscle tissues, is used. Myoglobin is a roughly spherical globular protein of 39 Å diameters [25] and is known to be a soft protein, likely to change its conformation at solid/liquid interfaces [26,27]. Experiments with circular dichroism and infrared spectroscopy have indeed shown changes in secondary structure but also in tertiary structure of myoglobin upon adsorption [28,29].

## 2. Materials and methods

### 2.1. Deuterated myoglobin solutions

The protein was deuterated and purified at the ILL Deuteration Laboratory using the procedure described in Ref. [30]. The protein used is a 100% deuterated myoglobin – the recombinant deuterated myoglobin was prepared in high cell density cultures using fully deuterated minimal medium with fully deuterated carbon source (d8-glycerol) [31,32]. From the amino acid sequence of the recombinant myoglobin we determined the total number of hydrogens (1381). 303 hydrogens (22%) out of the 1381 are bound to nitrogen, oxygen or sulfur and defined as “exchangeable”. Mass spectroscopy analysis has measured 21% of exchange, in good agreement with the estimation and another study previously published [33]. From this value, the scattering length density (SLD) of the deuterated myoglobin is  $6.75 \times 10^{-6} \text{ \AA}^{-2}$  in  $\text{H}_2\text{O}$  and  $7.21 \times 10^{-6} \text{ \AA}^{-2}$  in CMSi. Neutron crystallographic structure of fully deuterated myoglobin, do not show major differences with hydrogenated molecule [33], suggesting that deuterated myoglobin has, globally, the same properties than hydrogenated. All solutions were prepared with Milli-Q purified water (Millipore, Bedford, MA) with a resistivity of 18.2 MΩ cm in a 20 mM Tris and 50 mM NaCl Buffer at pH 7.5. The isoelectric point of myoglobin is 7.2 [25]. At pH 7.5 the protein can be considered as globally neutral.

### 2.2. Deposition of self assembled OTS layer

The silicon wafers were cleaned by using a “piranha solution” (1:3  $\text{H}_2\text{O}_2$ : $\text{H}_2\text{SO}_4$ ) for 10 min and were thoroughly rinsed afterwards with ion exchanged water. Self-assembled monolayers of OTS were formed on the substrates by immersing the clean silicon

wafers in a dichloromethane solution containing 1.5 mM of OTS for 4 h [34,35]. Since the grafting reaction is very sensitive to the amount of water in the environment [34], anhydrous dichloromethane was used and the reaction was carried out in a desiccator to minimize the uptake of water. Finally, samples were rinsed with dichloromethane to remove the excess of OTS. At this stage, the wafers were highly hydrophobic and ready to use for protein adsorption, as confirmed by contact angle measurements. The thicknesses of the deposited layers were measured by spectroscopic ellipsometry. The measurements were performed at least at 15 different positions on each sample. The thickness of the OTS layer was found between 23 Å and 26 Å depending on the sample. Four OTS substrates were prepared and immersed in solutions containing different protein concentrations. The substrates were labeled as function of the concentration; the codes OTS1, OTS05, OTS01 and OTS001 indicate samples that were respectively immersed in protein solutions of 1 mg/ml, 0.5 mg/ml, 0.1 mg/ml and 0.01 mg/ml.

### 2.3. Deposition of self assembled PS layer

For the substrate with a polystyrene (PS) layer, the wafers were treated for 30 min by ozone in a UV/ozone chamber (Bioforce UV/Ozone Procleaner) to remove molecular levels of contamination. A solution of 11 mg/ml vinyl-terminated PS ( $M_w = 2100 \text{ g/mol}$ , polydispersity  $M_w/M_n = 1.11$ ) (polymer sources) in chloroform was spread on the wafers and evaporated under a stream of nitrogen. The PS was grafted on the wafers by heating the samples at 150 °C in vacuum during three days in order to form covalent bonds between terminal vinyl groups and silicon [36]. The samples were rinsed with chloroform to remove the excess of polymers. At this stage, the wafers were hydrophobic and ready to use for protein adsorption. The samples were characterized by ellipsometry. The measurements were performed at least at 15 different positions for each sample. The thickness of the vinyl-terminated PS layer was found to be  $(30 \pm 3) \text{ \AA}$  and  $(35 \pm 5) \text{ \AA}$  for the two samples. As for OTS, the substrates were labeled as function of the concentration; the codes PS1 and PS001 indicate samples that were respectively immersed in protein solutions of 1 mg/ml and 0.01 mg/ml.

### 2.4. Neutron reflectivity

The NR measurements were performed at the Institut Laue-Langevin (ILL, Grenoble, France) using the D17 reflectometer [37] and at the Laboratoire Léon Brillouin (LLB, Saclay, France) using the EROS reflectometer [38]. In a neutron reflectivity experiment, specular reflection is measured as a function of the wave vector transfer perpendicular to the surface,  $q = (4\pi/\lambda)\sin\theta$ , where  $\theta$  is the angle and  $\lambda$  is the wavelength of the incident beam. The wavelength of the incident neutrons is between 2 Å and 20 Å both for D17 and EROS [37,38]. We used the time-of-flight configuration with the beam pulsed by a double chopper system with variable phase. Data were recorded at two or three fixed incident angles in order to cover the desired  $q$  range, and the resolution was around 4% at ILL and around 9% at LLB. The sample cell consisted of a PTFE reservoir containing the water solutions put against the silicon block sandwiched between two aluminum plates. At the ILL single-crystalline and polished silicon (111) substrates ( $5 \times 5 \times 1 \text{ cm}^3$ ) were used (Synchrotronix, France), while at the LLB round silicon crystals of 5.1 cm diameter and 0.5 cm thickness were used. The sample cells for both experiments were kept at a temperature of  $(25.0 \pm 0.5) \text{ }^\circ\text{C}$ . The contrast variation method was employed by using aqueous solutions of different scattering length densities by mixing  $\text{H}_2\text{O}$  and  $\text{D}_2\text{O}$ , allowing us to enhance the sensitivity of the measurements. The contrasts used were  $\text{D}_2\text{O}$ , CMSi, and  $\text{H}_2\text{O}$  with SLDs  $6.35 \times 10^{-6} \text{ \AA}^{-2}$ ,  $2.07 \times 10^{-6} \text{ \AA}^{-2}$  and  $-0.56 \times 10^{-6} \text{ \AA}^{-2}$ ,

CMSi is a contrast liquid that matches the silicon scattering length density. Data were analyzed by model fitting using the Parratt formalism [39,40]. The interface was described by a series of layers characterized by a thickness, a scattering length density and a roughness (the so-called box model). The contrasts for each measurement were fitted simultaneously to reduce the number of possible models describing the layer and so increase the resolution and confidence in the results.

### 2.5. Ellipsometry

Ellipsometry was used to determine the thickness and homogeneity of the hydrophobic OTS and PS layers prior to the neutron reflectivity experiments. The Horiba Jobin–Yvon MM-16 spectroscopic phase modulated ellipsometer was used. The ellipsometer consists of two light sources, a halogen and a LED lamp (430–850 nm). All the measurements were performed near the Brewster angle at an incidence of 70° and utilized the entire spectral range.

### 2.6. Contact angle measurement

Water contact angle (WCA) measurements were performed on a Krüss DSA 100 instrument. The contact angle was automatically measured using the Drop Shape analysis software provided by Krüss and the tangent method was used to determine the angles of contact. For each sample at least eight droplets were deposited at several different positions on each sample. The angles were measured on the two side of each droplet resulting in at least 16 measurements. The average of each measurement were then determined.

## 3. Results and discussion

The OTS and PS layers were characterized with NR in three different contrast liquids, H<sub>2</sub>O, D<sub>2</sub>O and CMSi. The reflectivity profiles measured as a function of momentum transfer  $q$  at the OTS (A) and PS (B) monolayer interface in D<sub>2</sub>O, CMSi and H<sub>2</sub>O are shown in Fig. 1. The points represent the experimental data and the lines show the fits. The systems were modeled using a series of slabs. The SLDs were fixed at  $2.07 \times 10^{-6} \text{ \AA}^{-2}$  for silicon,  $3.41 \times 10^{-6} \text{ \AA}^{-2}$  for silicon oxide,  $-0.44 \times 10^{-6} \text{ \AA}^{-2}$  for OTS and  $1.4 \times 10^{-6} \text{ \AA}^{-2}$  for PS. Tables 1 and 2 show the fitted parameters respectively for the OTS and PS wafers. The silicon oxide layer had thickness ranging from 9 Å and 14 Å, depending of the samples and contained from 3% to 25% of water. The water in the oxide layer is probably due to the porosity of the layer [41]. The values obtained are in good agreement with literature [35,42,43]. The OTS layer thickness was found

**Table 1**

Fitted parameters for the OTS layers as function of bulk concentration (thickness, % of the solvent, roughness). The roughness of the Si/SiO<sub>2</sub> is around 3 Å for all the samples. OTS1, OTS05, OTS01 and OTS001 correspond to the substrates later exposed to protein solutions of 1 mg/ml, 0.5 mg/ml, 0.1 mg/ml and 0.01 mg/ml concentration, respectively (see text).

	OTS1	OTS05	OTS01	OTS001
Thick SiO <sub>2</sub> (Å)	14 ± 2	10 ± 2	14 ± 1	13 ± 3
Sol SiO <sub>2</sub> (%)	24 ± 4	3 ± 2	25 ± 4	19 ± 5
Thick OTS (Å)	24 ± 1	26 ± 3	23 ± 2	22 ± 5
Rough SiO <sub>2</sub> /OTS (Å)	4 ± 1	2 ± 1	4 ± 2	10 ± 4

**Table 2**

Fitted parameters for the PS layers as function of bulk concentration (thickness, % of the solvent, roughness). The roughness of the Si/SiO<sub>2</sub> is around 2–3 Å for both samples. PS1 and PS001 correspond to the substrates later exposed to protein solutions of 1 mg/ml and 0.01 mg/ml concentration, respectively (see text).

	PS1	PS001
Thick SiO <sub>2</sub> (Å)	10 ± 2	9 ± 4
Sol SiO <sub>2</sub> (%)	21 ± 4	18 ± 9
Thick PS (Å)	32 ± 2	38 ± 4
Rough SiO <sub>2</sub> /PS (Å)	8 ± 2	6 ± 3

between 23 Å and 26 Å depending on the sample. These values are comparable to the length of the OTS molecule, known to be 24.3 Å [44], and in agreement with literature data [35,42,43,45]. The fitted parameters correspond to a surface excess of 7–7.9 μMol/m<sup>2</sup> and an area per molecule of 23.5–20.8 Å<sup>2</sup> indicating that the chains are densely packed [46]. Concerning the PS layers, their thicknesses were (32 ± 2) Å and (38 ± 4) Å. The fitted parameters correspond to a surface excess of 1.7 and 1.9 μMol/m<sup>2</sup> and an area per molecule of 100 Å<sup>2</sup> and 87 Å<sup>2</sup>, respectively. The surface excess values for PS are lower than for OTS since the molar mass is higher.

After the substrate characterization, the adsorption of proteins on the hydrophobic monolayers was performed using deuterated myoglobin solutions, at different protein concentrations. Four protein concentrations (1 mg/ml, 0.5 mg/ml, 0.1 mg/ml and 0.01 mg/ml) were used for the protein adsorption on OTS layers and two concentrations (1 mg/ml and 0.01 mg/ml) were used on the PS layers. After 6 h of immersion, the protein solutions were removed by rinsing with H<sub>2</sub>O, and the reflectivity profiles were measured. Since the protein was deuterated, the sensitivity to adsorbed protein was maximal in H<sub>2</sub>O contrast. However, the protein layers were also measured in CMSi at two concentrations (1 mg/ml and 0.1 mg/ml) on OTS and one concentration (1 mg/ml) on PS in order to increase the confidence of the fit. The measurements were performed on four OTS samples and two PS samples. Fig. 2 shows a

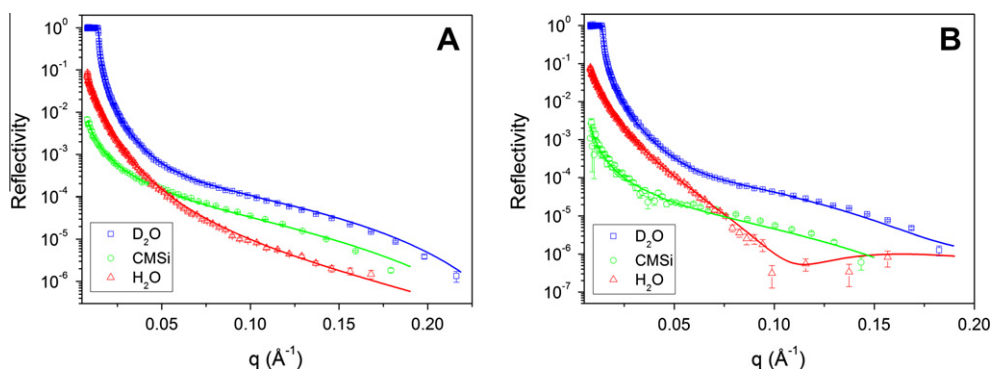


**Fig. 1.** Reflectivity profiles of the OTS1 (A) and for PS1 (B) in the three contrasts: (blue) D<sub>2</sub>O, (green) CMSi and (red) H<sub>2</sub>O. The lines are the fits to the data. (For interpretation of the references to color in this figure legend, the reader is referred to the web version of this article.)

comparison of the reflectivity profile from the H<sub>2</sub>O contrast, before and after the adsorption process for two different protein concentrations for OTS (A) and PS (B). For clarity, the profile for 0.5 mg/ml is not shown in the case of OTS. The reflectivity profile change after adsorption confirming the sensitivity of neutron reflectivity to protein adsorption: for the 0.01 mg/ml a minimum of the reflectivity curve is observed at around  $0.06 \text{ \AA}^{-1}$ , indicating the presence of a layer at the surface. Interestingly, for the sample exposed to a 1 mg/ml protein solution the reflectivity profile is more complex indicating a different structure on the surface (two minima are observed). Moreover, for each concentration a maximum is also observed between  $0.09 \text{ \AA}^{-1}$  and  $0.12 \text{ \AA}^{-1}$ . The change of reflectivity is also maximal in this region. During data analysis, the scattering length density values, the thickness and roughness of the substrate layers have been maintained constant. Since the grafting densities of the monolayers are high (see above), the monolayers are composed of closed packed molecules and the adsorption should not affect the substrate layer.

At low concentration (0.1 mg/ml and 0.01 mg/ml), one dense layer of about  $13 \text{ \AA}$  thick is necessary to fit the data and contains around 80% of protein. Myoglobin being a globular protein with a diameter of  $39 \text{ \AA}$  [25], this result indicates that the protein is denatured and flattened during the adsorption process – the protein architecture is broken and the molecule unfolds suggesting that the protein spreads its hydrophobic fragments (apolar amino acids) onto the hydrophobic OTS layer while the hydrophilic fragments composed of polar and charged amino acids are possibly on the top exposed to the bulk solution. Fig. 3 shows the scattering length density (SLD) profiles extracted from the fits for 1 mg/ml (1A) and 0.01 mg/ml (2A).

At high concentration (1 mg/ml and 0.5 mg/ml), a two-layer model is needed to fit the NR data: one inner layer close to the OTS layer and one outer layer on the top. The inner layer is about  $12 \text{ \AA}$  thick and it contains around a volume fraction 80% of protein as before while the outer layer is about  $40\text{--}50 \text{ \AA}$  thick and contains about 25% of volume fraction of myoglobin. The outer layer corresponds approximately to the protein dimension ( $39 \text{ \AA}$  diameters) and is quite rough ( $\sim 20 \text{ \AA}$ ). Fig. 3 shows also the SLD profile of this model (Fig. 1A and B). These results suggest that initially the proteins are adsorbed and denatured onto the OTS layer (same that at low concentration) and then another probably non-denatured protein layer is adsorbed on the top resulting in two adsorbed layers. Table 3 summarizes the fitted parameters from the data of the protein adsorption on the OTS layer for the different protein concentrations.

The thickness  $t$  and the protein volume fraction  $\Phi_{\text{Prot}}$  of the different protein layers allow us determining the amount of adsorbed protein  $\Gamma$  using the relation  $\Gamma = \Phi_{\text{Prot}} \rho t$ , where  $\rho = 1.34 \text{ g/cm}^3$  is

the myoglobin density [47]. In all cases, the adsorbed quantity of the first layer is around  $1.3 \text{ mg/m}^2$ . At high concentration, the second layer corresponds to about  $1.5 \text{ mg/m}^2$ . These values are also summarized in Table 3.

We also performed protein adsorption on PS self assembled monolayer in order to probe the effect of the substrate on the structure of the adsorbed layers. The reflectivity profiles are measured for myoglobin concentrations of 1 mg/ml and 0.01 mg/ml. The effect of the protein in H<sub>2</sub>O on the initial curve is shown in Fig. 2B. As in the case of the OTS substrate, the reflectivity is clearly sensitive to protein adsorption. At 0.01 mg/ml, data are fitted by one layer model of  $23 \text{ \AA}$  thick and containing 32% of protein. At 1 mg/ml, a two-layer model is needed: the inner layer is  $20 \text{ \AA}$  thick and it contains 46% solvent, while the outer layer is  $47 \text{ \AA}$  thick and contains 24% protein. The SLD profiles are shown in Fig. 3 while the parameters obtained from the fits are reported in Table 4.

The thickness,  $t$ , and the protein volume fraction,  $\Phi_{\text{Prot}}$ , of the different protein layers allow us to determine the amount of adsorbed protein  $\Gamma$ . At 1 mg/ml, the adsorbed quantity of the inner layer is  $(1.2 \pm 0.1) \text{ mg/m}^2$  and  $(1.5 \pm 0.2) \text{ mg/m}^2$  for the outer layer. At 0.01 mg/ml, the adsorbed quantity is  $(1.0 \pm 0.2) \text{ mg/m}^2$ . Those values are reported in Table 4. Fig. 4 summarizes the adsorbed amount as function of bulk concentration for OTS and PS. For OTS, from a bulk concentration of 0.5 mg/ml, the adsorbed amount increases due to the additional adsorbed protein layer at high concentration. While the adsorbed quantities are similar for OTS and PS, the protein layer thickness is different. Indeed the thickness of the inner layer is significantly higher on PS ( $\sim 21 \text{ \AA}$ ) than on OTS ( $\sim 12 \text{ \AA}$ ). This result indicates that myoglobin is significantly less flattened at the PS interface than at the OTS interface. This finding is in agreement with the lower degree of hydrophobicity of PS compared to OTS [48,49].

Adsorption of globular proteins at both hydrophilic and hydrophobic solid/liquid interfaces has been studied using a variety of experimental techniques. On a hydrophobic OTS surface, adsorption of  $\beta$ -lactoglobulin was studied with spectroscopic ellipsometry by Marsh et al. [50] and an adsorbed amount of  $1.7 \text{ mg/m}^2$  for a bulk concentration of 1 mg/ml was observed. This value is lower than the one found for myoglobin ( $2.6 \text{ mg/m}^2$ ). Since  $\beta$ -lactoglobulin has similar molecular weight and diameter than myoglobin, this result indicates that myoglobin has a greater affinity for OTS. This difference could also be associated with a possible lack (or less dense) of a second layer of adsorbed proteins. Ellipsometry cannot in general easily distinguish the structure of adsorbed layers. Nevertheless, protein adsorption consisting of two adsorbed layers was already observed. Neutron reflectometry was used by Fragneto et al. [42,51] for the study of  $\beta$ -casein and  $\beta$ -lactoglobulin adsorption on OTS as function of pH (8–3) at low

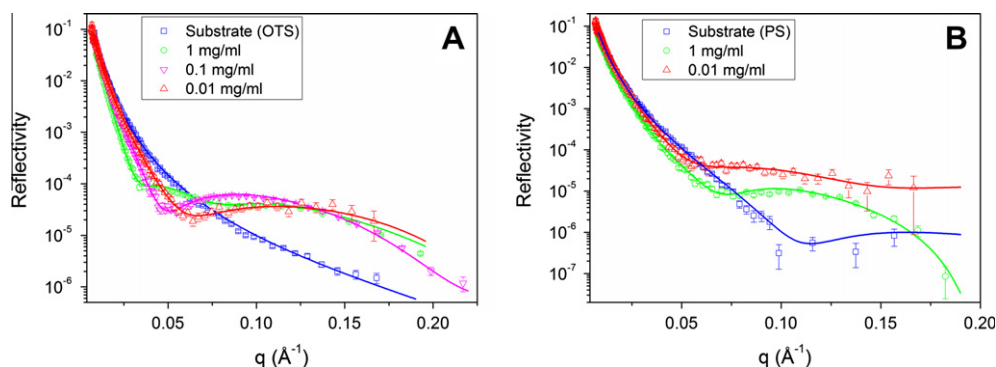
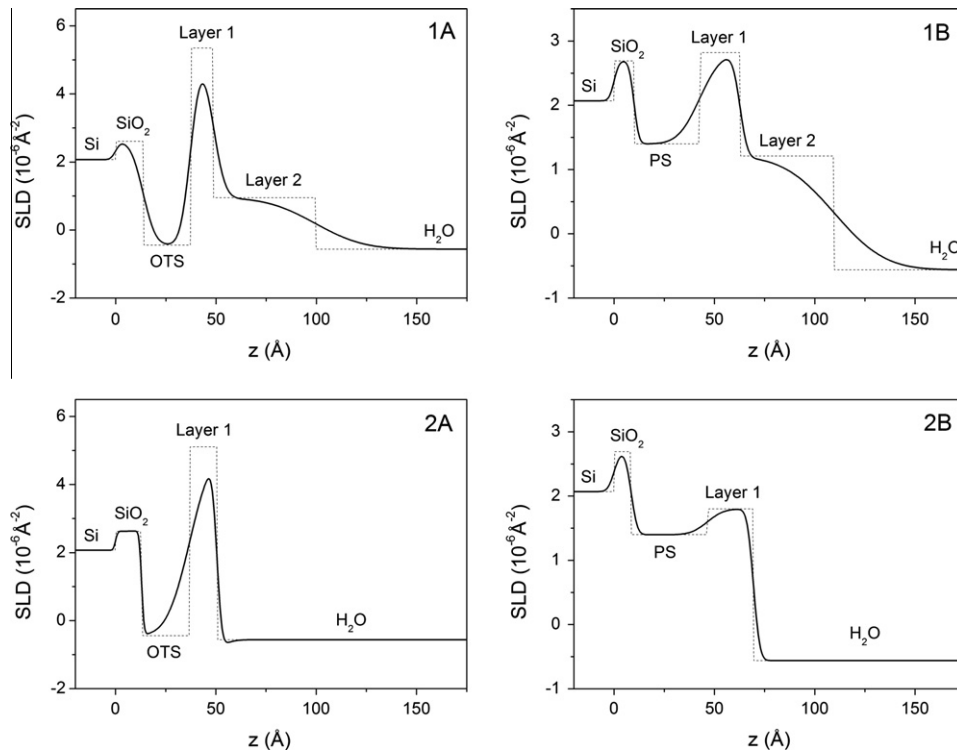


Fig. 2. Reflectivity profiles of OTS (A) and PS (B) before and after adsorption at bulk concentration of  $1 \text{ mg/m}^2$  and  $0.01 \text{ mg/m}^2$  in H<sub>2</sub>O contrast. The lines are the fits to the data.



**Fig. 3.** Density profile extracted from the fits for OTS (A) and PS (B) for 1 mg/ml (1) and 0.01 mg/ml (2). The dashed lines correspond to the profiles without layer roughness for comparison.

**Table 3**

Fitted parameters for the protein layers on OTS as function of bulk concentration. Thick is the thickness of the layer,  $\Phi_{\text{Prot}}$  is the volume fraction of the protein, rough prot 1 is the roughness between of the OTS layer and the first protein layer, rough prot 2 is the roughness between of the two protein layers,  $\Gamma_i$  is the adsorbed amount of layer  $i$  and  $\Gamma_{\text{total}}$  is the total adsorbed amount) OTS1, OTS05, OTS01 and OTS001 correspond to protein concentration of 1 mg/ml, 0.5 mg/ml, 0.1 mg/ml and 0.01 mg/ml, respectively (see text).

	OTS1	OTS05	OTS01	OTS001
Thick prot 1 (Å)	11 ± 1	13 ± 1	12.4 ± 0.5	13.5 ± 0.5
$\Phi_{\text{Prot1}}$ (%)	81 ± 2	83 ± 4	85 ± 3	77 ± 2
Rough prot 1 (Å)	5 ± 2	4 ± 3	5 ± 2	2 ± 1
$\Gamma_1$ (mg/m <sup>2</sup> )	1.2 ± 0.1	1.4 ± 0.2	1.4 ± 0.1	1.4 ± 0.1
Thick prot 2 (Å)	51 ± 7	38 ± 7	/	/
$\Phi_{\text{Prot2}}$ (%)	21 ± 2	34 ± 3	/	/
Rough prot 2 (Å)	19 ± 2	20 ± 3	/	/
$\Gamma_2$ (mg/m <sup>2</sup> )	1.4 ± 0.3	1.7 ± 0.5	/	/
$\Gamma_{\text{total}}$ (mg/m <sup>2</sup> )	2.6 ± 0.4	3.1 ± 0.7	1.4 ± 0.1	1.4 ± 0.1

**Table 4**

Fitted parameters for the protein layers on PS as function of bulk concentration (Thick is the thickness of the layer,  $\Phi_{\text{Prot}}$  is the volume fraction of the protein, rough prot 1 is the roughness between of the PS layer and the first protein layer, rough prot 2 is the roughness between of the two protein layers,  $\Gamma_i$  is the adsorbed amount in layer  $i$  and  $\Gamma_{\text{total}}$  is the total adsorbed amount). PS1 and PS001 correspond to protein solutions of 1 mg/ml and 0.01 mg/ml concentration, respectively (see text).

	PS1	PS001
Thick prot 1 (Å)	20 ± 1	23 ± 3
$\Phi_{\text{Prot1}}$ (%)	46 ± 1	32 ± 3
Rough prot 1 (Å)	3 ± 2	3 ± 2
$\Gamma_1$ (mg/m <sup>2</sup> )	1.2 ± 0.1	1.0 ± 0.2
Thick prot 2 (Å)	47 ± 3	/
$\Phi_{\text{Prot2}}$ (%)	24 ± 2	/
Rough prot 2 (Å)	20 ± 3	/
$\Gamma_2$ (mg/m <sup>2</sup> )	1.5 ± 0.2	/
$\Gamma_{\text{total}}$ (mg/m <sup>2</sup> )	2.7 ± 0.3	1.0 ± 0.2

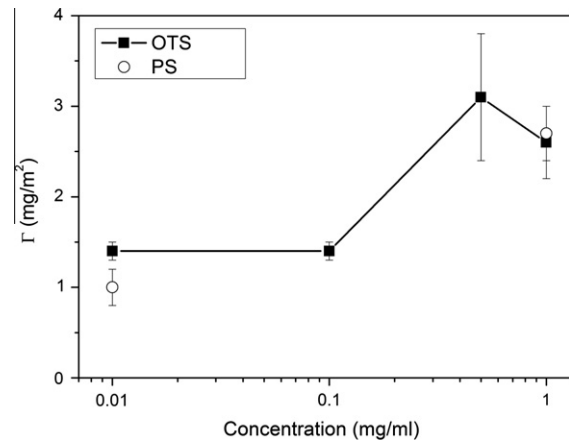


**Fig. 4.** Adsorbed quantity as function of myoglobin concentration solution on OTS (square) and PS (open circle) layers.

concentration (0.05 mg/ml).  $\beta$ -Casein has a structure composed of a polar head and a non-polar tail and it is a flexible protein while  $\beta$ -lactoglobulin is more compact [51]. Authors show that  $\beta$ -casein adsorption at pH 7 results in two-layer structure consisting of one dense layer of thickness 23 Å and a surface coverage of 1.9 mg/m<sup>2</sup> adjacent to the surface and an external layer protruding into the solution of thickness 35 Å and 12% protein volume fraction [42]. The protein is thus denatured at the interface. However, in this study, the second adsorbed layer was attributed to the hydrophilic segments of the denatured protein, which extend into the solvent. Furthermore  $\beta$ -lactoglobulin adsorption at pH 7 resulted in a single uniform layer of 32 Å. On hydrophilic surfaces, Marsh et al. showed with NR that  $\beta$ -lactoglobulin does not alter its

conformation and retains its native shape upon adsorption [45]. The denaturation of  $\beta$ -casein at hydrophobic interfaces was also confirmed by Follows et al. [52]. Moreover, Evers et al. shows a change of the denaturation of lysozyme with salt concentration leading to an improvement of the adsorption at high salt concentration [53]. Hahl et al. [54] have also shown by X-ray reflectivity that, at low concentration (0.1 mg/ml),  $\alpha$ -amylase, bovin serum albumin (BSA) and lysozyme are denaturated on hydrophobic surfaces and not denaturated on hydrophilic  $\text{SiO}_2$ . Lu et al. [41] also studied lysozyme adsorption on OTS as function of pH at a low protein concentration of 0.03 mg/ml. They also show denaturation of the protein at the interface with a dense sub-layer of 12–15 Å and a loose diffuse layer of some 50 Å. Again, the outer layer is not attributed to an additional protein layer but to expulsion of polar amino acids to the solvent.

In our case, for low concentration only a thin and dense layer is observed, while for higher density a two-layer structure is detected. This result suggests that myoglobin presents a higher degree of denaturation at a hydrophobic surface than  $\beta$ -lactoglobulin,  $\beta$ -casein and lysozyme. Indeed, myoglobin is known as a soft and flexible protein and is thus able to be denaturated at solid/liquid interfaces. Experiments with circular dichroism and infrared spectroscopy have shown a change in secondary structure but also in tertiary structure of myoglobin upon adsorption [28,29].

The protein being fully deuterated, the sensitivity to the layer structure is high. For the low concentration we estimated that a layer of protein volume fraction of 4% or higher could be detected easily, indicating that at low concentration the film structure is mainly formed by a thin and dense protein layer of around 13 Å on OTS and 22 Å on PS.

To further discuss the results, measurements of water contact angle (WCA) were performed. On a bare silicon substrate the contact angle was found to be  $29^\circ \pm 8^\circ$  while it was  $11^\circ \pm 1^\circ$  after piranha cleaning indicating the piranha process is efficient. The contact angle after OTS and PS grafting were  $110^\circ \pm 3^\circ$  and  $96^\circ \pm 3^\circ$ , respectively for OTS and PS as expected for hydrophobic samples. These results are in agreement with literature [48,49]. After immersion of the samples in protein solution in the same conditions as used for neutron reflectivity experiments and using hydrogenated myoglobin (Sigma Aldrich), the WCA measurements give for OTS a contact angle of  $59^\circ \pm 9^\circ$  and  $56^\circ \pm 8^\circ$  for myoglobin concentrations of 1 mg/ml and 0.01 mg/ml respectively. In the case of PS, the contact angles found are  $67^\circ \pm 6^\circ$  and  $50^\circ \pm 9^\circ$ , for myoglobin concentrations of 1 mg/ml and 0.01 mg/ml, respectively. These measurements confirm that the adsorbed protein layers make indeed the surface partially hydrophilic.

#### 4. Conclusions

The adsorption of proteins on hydrophobic surfaces has been studied using neutron reflectivity combined with deuterated protein. Deuterated myoglobin was adsorbed on hydrophobic surfaces from OTS and PS at different concentrations. At low concentration, the protein forms one thin layer of thickness well below the native dimensions of the protein. This indicates that the protein is denaturated at the hydrophobic interface. Moreover, water contact angle measurements show that the adsorbed protein layers make the substrates hydrophilic, suggesting that adsorbed proteins spread their hydrophobic fragments onto the hydrophobic substrate while the hydrophilic fragments (polar and charged amino acid) remain exposed to water. On the PS substrate, the adsorbed layer is thicker than on OTS indicating that the protein is significantly less flattened on PS. At high concentration, one additional nondenaturated layer is observed on the top of the first layer.

Results from this work provide a proof not only of the effect of different (although with very similar properties) substrates to protein adsorption but also on the difficulty to extract general rules on adsorption phenomena when biological molecules are concerned and the importance to study adsorption behavior for individual systems of interest. Proteins with similar shape, mass and size can have different adsorption properties even on uncharged surfaces (see the discussed comparison between myoglobin and  $\beta$ -lactoglobulin adsorption behavior). This confirms the complexity of this phenomenon of outstanding importance in the field of bio-fouling in general.

#### Acknowledgments

The authors acknowledge funding of FNRS of Belgium via FRFC. ILL and LLB are thanked for the beam allocation. We would like to thank Luca Signor from the Mass Spectrometry Platform at the IBS in Grenoble for sample analysis.

#### References

- [1] J.L. Brash, T.A. Horbett (Eds.), *Proteins at Interfaces II*, 602, ACS, Washington, DC, 1995.
- [2] R.A. Silva, M.D. Urzua, D.F.S. Petri, P.L. Dubin, *Langmuir* 26 (2010) 14032.
- [3] W. Norde, *Adv. Colloid Interface Sci.* 29 (1990) 267.
- [4] M. Rabe, D. Verdes, S. Seeger, *Adv. Colloid Interface Sci.* 162 (2011) 87.
- [5] J.D. Andrade, V. Hlady, *Adv. Polym. Sci.* 79 (1986) 1.
- [6] T.J. Su, J.R. Lu, R.K. Thomas, Z.F. Cui, J. Penfold, *J. Phys. Chem. B* 41 (1998) 8100.
- [7] T. Ekblad, B. Liedberg, *Curr. Opin. Colloid Interface Sci.* 15 (2010) 499.
- [8] T.J. Su, J.R. Lu, R.K. Thomas, Z.F. Cui, *J. Phys. Chem. B* 103 (1999) 3727.
- [9] T.J. Su, J.R. Lu, R.K. Thomas, Z.F. Cui, J. Penfold, *J. Colloid Interface Sci.* 219 (1999) 419.
- [10] T.J. Su, J.R. Lu, R.K. Thomas, Z.F. Cui, J. Penfold, *Langmuir* 14 (1998) 438.
- [11] F. Evers, K. Shokuie, M. Paulus, C. Sternemann, C. Czeslik, M. Tolan, *Langmuir* 24 (2008) 10216.
- [12] A. Quinn, H. Mantz, K. Jacobs, M. Bellion, L. Santen, *EPL* 81 (2008) 56003.
- [13] A. Halperin, *Langmuir* 15 (1999) 2525.
- [14] A. Halperin, G. Fragneto, A. Schollier, M. Sferrazza, *Langmuir* 23 (2007) 10603.
- [15] F. Fang, J. Satulovsky, I. Szeleifer, *Biophys. J.* 89 (2005) 1516.
- [16] E.P.K. Currie, J. Van der Gucht, *Pure Appl. Chem.* 71 (1999) 1227.
- [17] W. Bosker, P. Iakovlev, W. Norde, M.C. Stuart, *J. Colloid Interface Sci.* 286 (2005) 496.
- [18] W. Norde, D. Gage, *Langmuir* 20 (2004) 4162.
- [19] W. Senaratne, L. Andruzzi, C.K. Ober, *Biomacromolecules* 6 (2005) 2427.
- [20] U. Jönsson, B. Ivarsson, I. Lundström, L. Berghem, *J. Colloid Interface Sci.* 90 (1982) 148.
- [21] B.R. Murphy, M.A. Phelan, D.L. Nelson, R. Yarchoan, E.L. Tierney, D.W. Alling, R.M. Chanock, *J. Clin. Microbiol.* 13 (1981) 554.
- [22] C.R. Daniels, C. Reznik, R. Kilmer, M.J. Felipe, M. Celeste, R. Tria, K. Kourentzi, W.-H. Chen, R.C. Advincula, R.C. Willson, C.F. Landes, *Colloids Surf. B* 88 (2011) 31.
- [23] P. Roach, D. Farrar, C.C. Perry, *J. Am. Chem. Soc.* 127 (2005) 8168.
- [24] J.R. Lu, X. Zhao, M. Yaseen, *Curr. Opin. Colloid Interface Sci.* 12 (2007) 9.
- [25] L. Stryer, in: *Biochemistry*, W.H. Freeman International Student Edition, 1981.
- [26] A. Kondo, J. Mihara, *J. Colloid Interface Sci.* 177 (1996) 214.
- [27] M. Iafisco, B. Palazzo, G. Falini, M. Di Foggia, S. Bonora, S. Nicolis, L. Casella, N. Roveri, *Langmuir* 24 (2008) 4924.
- [28] H. Wu, Y. Fan, J. Sheng, S.-F. Sui, *EPJ* 22 (1993) 201.
- [29] A. Kondo, F. Murakami, K. Higashitani, *Biotechnol. Bioeng.* 40 (1992) 889.
- [30] R. Burgess, *Protein purification*, in: H.G. Nothwang, S.E. Pfeiffer (Eds.), *Proteomics of the Nervous System*, Wiley-VCH Verlag GmbH and Co, 2008.
- [31] J.-B. Artero, M. Haertlein, S. McSweeney, P. Timmins, *Acta Cryst.* 61 (2005) 1541.
- [32] I. Hazemann, M.T. Dauvergne, M.P. Blakeley, F. Meilleur, M. Haertlein, A. Van Dorsseleer, A. Mitschler, D.A.A. Myles, A. Podjarny, *Acta Cryst.* 61 (2005) 1413.
- [33] F. Shu, V. Ramakrishnan, B.P. Schoenborn, *PNAS* 97 (2000) 3872.
- [34] P. Silberzan, L. Leger, D. Ausserre, J.J. Benattar, *Langmuir* 7 (1991) 1647.
- [35] G. Fragneto, J.R. Lu, D.C. McDermott, R.K. Thomas, A.R. Rennie, P.D. Gallagher, S.K. Satija, *Langmuir* 12 (1996) 477.
- [36] J.H. Maas, M.A. Stuart, A.B. Sieval, H. Zuilhof, *Thin Solid Films* 426 (2003) 135.
- [37] R. Cubitt, G. Fragneto, *Appl. Phys. A* 74 (2002) 329.
- [38] F. Cousin, F. Ott, F. Gibert, A. Menelle, *Eur. Phys. J. Plus* 126 (2011) 1.
- [39] L.G. Parratt, *Phys. Rev.* 95 (1954) 359.
- [40] T.P. Russell, *Mater. Sci. Rep.* 5 (1990) 171.
- [41] J.R. Lu, T.J. Su, P.N. Thirtle, R.K. Thomas, A.R. Rennie, R. Cubitt, *J. Colloid Interface Sci.* 206 (1998) 212.
- [42] G. Fragneto, R. Thomas, A. Rennie, J. Penfold, *Science* 267 (1995) 657.
- [43] D.C. McDermott, J.R. Lu, E.M. Lee, R.K. Thomas, A.R. Rennie, *Langmuir* 8 (1992) 1204.

- [44] I.M. Tidswell, B.M. Ocko, P.S. Pershan, S.R. Wasserman, G.M. Whitesides, J.D. Axe, *Phys. Rev. B* 41 (1990) 1111.
- [45] R.J. Marsh, R.A.L. Jones, M. Sferrazza, J. Penfold, *Interface Sci.* 218 (1999) 347.
- [46] M. Fujii, S. Sugisawa, K. Fukada, T. Kato, T. Seimiya, *Langmuir* 11 (1995) 405.
- [47] S. Katz, J. Denis, *Biochim. Biophys. Acta* 207 (1970) 331.
- [48] M.E. McGovern, K.M.R. Kallury, M. Thompson, *Langmuir* 10 (1994) 3607.
- [49] Y. Li, J.Q. Pham, K.P. Johnston, P.F. Green, *Langmuir* 23 (2007) 9785.
- [50] R.J. Marsh, R.A.L. Jones, M. Sferrazza, *Colloids Surf. B* 23 (2002) 31.
- [51] G. Fragneto, T.J. Su, J.R. Lu, R.K. Thomas, A.R. Rennie, *Phys. Chem. Chem. Phys.* 2 (2000) 5214.
- [52] D. Follows, C. Holt, R.K. Thomas, F. Tiberg, G. Fragneto, T. Nylander, *Food Hydrocolloids* 25 (2011) 724.
- [53] F. Evers, K. Shokuie, M. Paulus, S. Tiemeyer, Ch. Sternemann, C. Czeslik, M. Tolan, *EPJST* 167 (2009) 185.
- [54] H. Hahl, F. Evers, S. Grandthyll, M. Paulus, C. Sternemann, P. Loskill, M. Lessel, A.K. Hüsecken, T. Brenner, M. Tolan, K. Jacobs, *Langmuir* 28 (2012) 7747.